Activities in Aqueous Solutions of the Alkali Halide Salts from Molecular Simulation

Maximilian Kohns, Michael Schappals, Martin Horsch,* and Hans Hasse

Laboratory of Engineering Thermodynamics, University of Kaiserslautern, Erwin-Schrödinger Str. 44, D-67663 Kaiserslautern, Germany

E-mail: martin.horsch@mv.uni-kl.de

Abstract

Activities of the alkali halide salts in aqueous solution are systematically investigated by molecular simulation of alkali halide salt solutions, using a set of ion models developed in previous work of our group in combination with SPC/E water. Five cations and four anions are considered (Li^+, Na^+, K^+, Rb^+, Cs^+, and F^-, Cl^-, Br^-, I^-). All 19 combinations of these ions to salts which are soluble in water are investigated (only LiF is insoluble in water). These models were not adjusted to activity data so that the present results are predictions. The OPAS method, which employs a virtual semipermeable membrane, is used to compute the activity data. The predictions are compared to experimental data. While for salts of the larger ions mostly good predictions are observed, there are important deviations in several of the other systems. A multicriteria approach for including the activity data in the model development is presented.

*To whom correspondence should be addressed

1 Introduction

Among the various thermodynamic properties of electrolyte solutions, the salt activity coefficient and the solvent activity belong to the most important ones. They determine phase equilibria, such as the salt solubility, the vapor pressure lowering, and the freezing point depression. For aqueous solutions of electrolytes, a large number of experimental studies on activity coefficients or related properties exists in the literature, most of which are based on measurements of the solvent activity. Many of these data have been correlated empirically by Hamer and Wu.[1] As the behavior of electrolyte solutions is difficult to describe due to solvation effects and the long-range Coulombic interactions of the charged species with each other and also with the solvent, such correlations usually employ a large number of parameters.

Molecular simulation provides an interesting alternative to this approach. By explicitly considering the interactions between all components on the molecular level, the long-range electrostatic effects and solvation phenomena in the electrolyte solution are intrinsically captured. The quality of molecular simulation results solely depends on the quality of the used molecular models.

Many ion models for describing properties of aqueous electrolyte solutions have been reported in the literature. We use the term ion model set for a set of m anion and n cation models which is designed for describing all $m \times n$ salts which can be formed by these ions. For a detailed discussion, see the recent review by Nezbeda et al. [2]. We focus here on Lennard-Jones (LJ) based ion models. Alkali and halide ion models of that type are described e.g. in.[3–11] The parameterization strategies employed in the development of these models differ strongly. E.g. Reiser et al.[11] developed their alkali and halide ion model set mainly based on density data, which was complemented by transport and structural data. Obtaining reliable activity data from molecular simulation is demanding, and it is only sometimes used in model development or refinement.[6–9,12–14]

There are several molecular simulation studies on activity data in aqueous solution.[15–26] In

most cases, only NaCl was studied. A recent study by Mester and Panagiotopoulos[27] considers four salts (NaF, NaCl, NaI, KCl) with three or four tested ion model sets per salt.

We present here for the first time a comprehensive study of activity data of aqueous solutions of all alkali halide salts (with the exception of LiF, which is practically insoluble in water). The ion model set of Reiser et al. is used[11] in combination with SPC/E water.[28] For describing a wide variety of properties of aqueous solutions of 19 different salts, only 10 adjustable parameters are used. That ion model set has been shown to give good results for many different properties of aqueous and also methanolic and ethanolic electrolyte solutions.[29,30] Since no activity coefficients or related properties were incorporated in the model development, all simulation results of the present study are strict predictions and serve as a further test of the performance of the models. The models were optimized with respect to properties at low to intermediate salt concentrations. The simulations of the present study are therefore carried out up to a molality of about $m = 2.5$ mol kg^{-1}.

The employed computational method (OPAS,[31] osmotic pressure for the activity of the solvent) provides results for the water activity. The salt activity coefficients are derived from the water activity results using the Gibbs-Duhem equation.

The paper is structured as follows: The molecular models and simulation methods are described in Section 2. The simulation results are presented and discussed in Section 3, and are used to illustrate a strategy for further model development for electrolyte solutions. Section 4 summarizes the main findings.

2 Molecular Models and Simulation Method

2.1 Molecular Models

In this study, the alkali and halide ions are modeled as single LJ sites with point charges in the center of the LJ site. The set of ion model parameters is taken from previous work of our group.[11] It is intended for use together with the SPC/E water model.[28] The ion model

parameters are given in Table 1.

[Table 1 about here.]

The ion models are combined with SPC/E water[28] throughout the present work. The total energy of the system writes as

$$\begin{aligned} U &= U_{\mathrm{LJ}} + U_{\mathrm{C}} \\ &= \sum_{i=1}^{N-1} \sum_{j=i+1}^{N} \left\{ \sum_{a=1}^{n_i^{\mathrm{LJ}}} \sum_{b=1}^{n_j^{\mathrm{LJ}}} 4\epsilon_{ijab} \left[\left(\frac{\sigma_{ijab}}{r_{ijab}} \right)^{12} - \left(\frac{\sigma_{ijab}}{r_{ijab}} \right)^{6} \right] \right. \\ &\quad \left. + \sum_{c=1}^{n_i^e} \sum_{d=1}^{n_j^e} \frac{1}{4\pi\varepsilon_0} \frac{q_{ic} q_{jd}}{r_{ijcd}} \right\}, \end{aligned} \tag{1}$$

where the indices a, b, c, and d refer to model interaction sites and i and j refer to molecules (including ions), ε_0 is the vacuum permittivity, ϵ_{ijab} and σ_{ijab} are the Lennard-Jones energy and size parameters, r_{ijab} and r_{ijcd} are site-site distances, and q_{ic} and q_{jd} are the magnitude of the point charges. The interaction between unlike LJ sites is described by the Lorentz-Berthelot combining rules[32,33]

$$\sigma_{ijab} = \frac{\sigma_{iiaa} + \sigma_{jjbb}}{2}, \tag{2}$$

$$\epsilon_{ijab} = \sqrt{\epsilon_{iiaa} \epsilon_{jjbb}}. \tag{3}$$

2.2 Simulation Method

The OPAS method is used to determine solvent activities and solute activity coefficients. The method is described in detail in a previous publication[31] and is only briefly summarized here. The simulation scenario is based on the general idea of Murad and Powles [34] and

has previously been used by others to refine existing models for some specific salts with respect to the osmotic pressure [12–14]. OPAS molecular dynamics simulations employ two virtual membranes in the simulation box which are permeable for the solvent, but not for the solute. In equilibrium, the solvent chemical potentials in the solution phase and the pure solvent phase must be equal, which can only be achieved by a pressure difference, the osmotic pressure Π. By sampling the force on the membranes, the osmotic pressure is computed. It is directly related to the solvent activity via

$$\ln a_{\mathrm{solv}} = -\frac{\Pi}{\rho_{\mathrm{solv}} RT}, \tag{4}$$

where R is the universal gas constant, and ρ_{solv} is the molar density of the pure liquid solvent at the temperature T, which is assumed to be independent of pressure. In the present work, the density $\rho_{\mathrm{SPC/E}} = 55.27$ mol l^{-1} of pure SPC/E water at $T = 298.15$ K and $p = 1$ bar is taken from Guevara-Carrión et al.[35] The idea of computing the solvent activity from simulations of the osmotic pressure was recently also mentioned by Smith et al. [36].

The chemical potential of a 1-1 electrolyte CA in aqueous solution, which dissociates into the ions C^+ and A^-, is usually expressed as

$$\mu_{\mathrm{CA}} = \mu^0_{\mathrm{CA}} + 2RT \ln(m_{\mathrm{CA}}/m_0) + 2RT \ln \gamma_{\mathrm{CA}}, \tag{5}$$

where μ^0_{CA} is the reference chemical potential of the Henry-like normalization, m_{CA} is the salt molality, and γ_{CA} is the salt activity coefficient. Hamer and Wu[1] presented correlations of experimental data for the activity coefficients of several 1-1 electrolytes in aqueous solution of the form

$$\ln \gamma_{\mathrm{CA}} = \ln(10) \left(\frac{-A\sqrt{m_{\mathrm{CA}}/m_0}}{1 + B\sqrt{m_{\mathrm{CA}}/m_0}} + \beta \frac{m_{\mathrm{CA}}}{m_0} + C \left(\frac{m_{\mathrm{CA}}}{m_0} \right)^2 \right), \tag{6}$$

which is a empirical extension of Debye-Hückel theory. Here, $m_0 = 1$ mol kg^{-1}, and B, β and C are dimensionless fit parameters. For some of the highly soluble salts, additional

polynomial terms involving higher powers of the salt molality m_{CA} are introduced. The parameter A is given by Debye-Hückel theory and only depends on the relative permittivity of the solvent ε and the temperature T:

$$A = \frac{1.824 \times 10^6}{(\varepsilon T/T_0)^{3/2}}, \tag{7}$$

where $T_0 = 1$ K so that A is dimensionless. In the present study, the value $A = 0.5677$ for SPC/E water at $T = 298.15$ K given by Mester and Panagiotopoulos[27] is used, corresponding to $\varepsilon = 73$.

The chemical potential of the solvent water is expressed by a normalization according to Raoult

$$\mu_{\mathrm{W}} = \mu_{\mathrm{W}}^0 + RT \ln a_{\mathrm{W}}, \tag{8}$$

where a_{W} is the water activity. The expression for a_{W} is found from Eqs. (5) and (6) using the Gibbs-Duhem equation (treating the salt as a single component):

$$\begin{aligned} \ln a_{\mathrm{W}} = &- 2M_{\mathrm{W}} \frac{m_{\mathrm{CA}}}{m_0} - M_{\mathrm{W}} \ln(10) \Bigg(\beta \Big(\frac{m_{\mathrm{CA}}}{m_0} \Big)^2 + \frac{4}{3} C \Big(\frac{m_{\mathrm{CA}}}{m_0} \Big)^3 \\ &+ \frac{2A}{B^3 + B^4 \sqrt{m_{\mathrm{CA}}/m_0}} + \frac{4A \ln(B\sqrt{m_{\mathrm{CA}}/m_0} + 1)}{B^3} \\ &- \frac{2A\sqrt{m_{\mathrm{CA}}/m_0}}{B^2} - \frac{2A}{B^3} \Bigg) \end{aligned} \tag{9}$$

The OPAS method provides results for the water activity $\ln a_{\mathrm{W}}$ depending on the salt molality m_{CA}. By fitting the parameters in Eq. (9) to the OPAS results, a correlation for $\ln a_{\mathrm{W}}$ is obtained. Eq. (6) then yields a thermodynamically consistent representation of the salt activity coefficient. Since only concentrations $m_{\mathrm{CA}} < 2.5$ mol kg^{-1} are investigated in the present work, it is sufficient to consider only the parameters B, β and C in the correlations

when fitting the simulation results.

All simulations of this study were carried out with an extended version of the molecular simulation program $ms2$.[37] Simulation details are given in Appendix A.

3 Results and Discussion

3.1 Investigation of Current Models

For all 19 alkali halide salts, OPAS simulations of aqueous solutions were carried out for different salt concentrations and $T = 298.15$ K. The simulation results were used to fit correlations according to Eq. (9) for the water activity and the fit parameters were transferred to the expression for the salt activity coefficient, cf. Eq. (6). These correlations are valid up to the highest simulated molality, which is $m_{\mathrm{CA}} \approx 2.5$ mol kg^{-1} in all cases (except for NaF, which is only soluble up to $m_{\mathrm{NaF}} \approx 1.0$ mol kg^{-1}). The fit parameters are given in Table 2 and the comparisons between simulation results and the correlations to experimental data are shown in Figs. 1 to 5. The numerical simulation results are reported in the Supporting Information.

[Table 2 about here.]

[Figure 1 about here.]

[Figure 2 about here.]

[Figure 3 about here.]

[Figure 4 about here.]

[Figure 5 about here.]

For four of the salts, namely NaF, NaCl, NaI, and KCl, simulation results have recently been reported by Mester and Panagiotopoulos[27] using the same molecular models, but a different simulation method. In all four cases, good agreement is observed between the results of Mester and Panagiotopoulos and the present simulation results, which serves as a mutual validation of both computational methods.

The statistical uncertainty for the salt activity coefficients obtained with the OPAS method is illustrated here for the case of KCl. It was obtained by fitting correlations to the disturbed simulation results $\ln a_{\mathrm{W}} \pm \Delta \ln a_{\mathrm{W}}$, where $\Delta \ln a_{\mathrm{W}}$ is the uncertainty in the water activity, defined as the standard deviation obtained with the block average method by Flyvbjerg and Petersen.[38] Thereby, the red dotted curves in the $\ln \gamma_{\mathrm{KCl}}$ panel of Fig. 3 are obtained. At the highest investigated concentration, they differ about ± 0.05 from the original correlation. This is similar to the standard deviation of the simulation results reported by Mester and Panagiotopoulos, which is ± 0.04 in this concentration range. Both methods therefore provide results with similar accuracy.

In the following, we briefly summarize some findings from the comparison of the simulation results (red dashed lines) and the correlations of experimental data (black solid lines) in Figs. 1 to 5. While the agreement between the predictions and the experimental data seems to be fair in most cases for the water activity, the results for the salt activity coefficient show larger deviations, which shows that the activity coefficient of the salt is a much more sensitive property than the activity of water. In assessing the deviations it should be considered that the simulation results are predictions from a very simple model with only 10 adjustable parameters, which were basically determined using density data alone. Still, the trends are always predicted correctly. The predictions for the bromides and iodides match the experimental data astonishingly well.

One exception to this are the sodium halides. A possible reason for this may be that the ion size parameters were obtained by fitting to the density of aqueous solutions,[10] which are very similar for the lithium and sodium halides. As a result, the lithium and sodium ion

size parameters are almost identical, cf. Table 1. In contrast, the activity coefficient curves for the lithium and sodium halides are significantly different. Consequently, the activity coefficient predictions for one of the two cations are expected to show better agreement with experimental data than for the other. From Figs. 1 and 2 it is clear that this is the case: the lithium salts show a better overall performance than the sodium salts.

The predictions for the alkali fluorides, however, deviate significantly from the experimental data. One exception is NaF, which shows fair agreement up to its low solubility limit. At this point it is interesting to note that Fyta et al.[7–9] had to overcome various obstacles when trying to adjust their ion model set to activity coefficients of the fluoride salts (especially NaF and KF) with Kirkwood-Buff theory. The model results would only match the experimental data after introducing scaling factors in the Lorentz-Berthelot mixing rules. In general, the alkali fluorides seem to be much harder to describe well than salts with larger anions, for which the investigated ion model set yields much better results.

As a further check of the model performance as well as the OPAS simulation methodology in general, simulations of aqueous NaCl solutions were carried out at T = 473.15 K and a pressure of p = 15.5 bar in the pure solvent phase. For this system, simulation results were recently reported by Mester and Panagiotopoulos [27], which again enables a mutual validation of the two computational approaches. The simulation results are presented in Fig. 6 and compared to the reference data of Pitzer et al.[39], and the numerical values are tabulated in the Supporting Information.

[Figure 6 about here.]

Good agreement is obtained between the simulation results by Mester and Panagiotopoulos and the OPAS simulations of the present work for this elevated temperature as well. The fit parameters to the OPAS simulation results are B = 2.2841, β = -0.016 and C = 0.0158; and A = 0.9349 was again taken from the relative permittivity values of Mester and Panagiotopoulos [23]. The activity coefficient of NaCl is still overestimated, but is closer to the experimental reference data than for T = 298.15 K. However, the trend of the experimen-

tal data is again captured well, so that a model refinement could possibly lead to a better agreement with experimental data.

In summary, the quality of the predictions of the ion model set of Reiser et al.[11] is encouraging, given the fact that the models were parameterized mainly using density data. Activity data of salts comprising large ions are generally represented well, while salts involving smaller ions show larger deviations from experimental data, so that there is ample room for improvements. Therefore, the development of new ion model sets with including data on activity coefficients should be pursued. The following section proposes a strategy to incorporate the OPAS simulation results in this process.

3.2 Use of Results for Model Development

The results obtained in the simulations discussed above can also be seen as a systematic investigation of a model class in general, i.e. charged LJ sites, in mixtures with the SPC/E water model. This model class possesses four LJ parameters for the ions $(\sigma_{\mathrm{C}}, \sigma_{\mathrm{A}}, \epsilon_{\mathrm{C}}, \epsilon_{\mathrm{A}})$. Following Reiser et al.,[11] the energy parameters $\epsilon_{\mathrm{C}}/k_{\mathrm{B}} = \epsilon_{\mathrm{A}}/k_{\mathrm{B}} = 200$ K are not varied here, so that the parameter space for a given salt has two dimensions $(\sigma_{\mathrm{C}}, \sigma_{\mathrm{A}})$. The present correlations for $\ln a_{\mathrm{W}}$ for all investigated ion combinations, i.e. grid points in the $(\sigma_{\mathrm{C}}, \sigma_{\mathrm{A}})$ parameter space, were interpolated bilinearly between the model parameter values from Reiser et al.[11] This enables estimating the water activity curve $\ln a_{\mathrm{W}} = \ln a_{\mathrm{W}}(\sigma_{\mathrm{C}}, \sigma_{\mathrm{A}}, m_{\mathrm{CA}})$ for any possible ion size parameter combination and salt molality. This can be used for model development.

As an example, the development of a new KF model is considered here. Two objective functions are used. The first objective function is the mean square deviation of the water activity curve, which is defined as

$$\delta \ln a_{\mathrm{W}} = \sqrt{\frac{1}{N-1} \sum_{i=1}^{N} \left(\frac{\ln a_{\mathrm{W}}^{\mathrm{exp}}(m_i) - \ln a_{\mathrm{W}}^{\mathrm{sim}}(m_i)}{\ln a_{\mathrm{W}}^{\mathrm{exp}}(m_i)} \right)^2}, \tag{10}$$

where N is the number of molalities for which the correlations are interpolated and the exponents 'exp' and 'sim' denote the values obtained from the Hamer and Wu correlations and the interpolation of OPAS results, respectively. Here, the OPAS correlations were extrapolated up to $m_N = 2.5$ mol kg^{-1}. The property $\delta \ln a_{\mathrm{W}}$ is evaluated on a 41×41 grid in the $(\sigma_{\mathrm{C}}, \sigma_{\mathrm{A}})$ parameter space.

The second objective function to be minimized is the deviation of the slope of the density of the aqueous electrolyte solution, which is defined as

$$\delta b = \sqrt{\left(\frac{b^{\mathrm{exp}} - b^{\mathrm{sim}}}{b^{\mathrm{exp}}} \right)^2}, \qquad \text{where } b = \left(\frac{\partial \rho}{\partial x_{\mathrm{Ion}}} \right)_{T,p}. \tag{11}$$

It was found by Reiser et al.[40] that the density of aqueous alkali halide solutions depends almost linearly on the ion mole fraction. The density simulation results of Reiser et al.[40] were used as the basis for interpolation on the same 41×41 grid as for the water activity data. Note that these results have to be rescaled to the molecular mass of KF.

The results of the computation of the deviations as a function of the model parameters $(\sigma_{\mathrm{C}}, \sigma_{\mathrm{A}})$ are shown as contour plots in Fig. 7.

[Figure 7 about here.]

Fig. 7 underlines that the molecular model for KF by Reiser et al.[11] shows, as expected, good performance for the density, while it gives poor results for the water activity. Fig. 7 also includes information on the valleys of lowest ascent/descent in the deviation contour plots (white lines). For the two objective functions considered here, these valleys go in different directions, which underlines that the objective functions 'water activity curve' and 'slope of the density' are conflicting targets. However, there is an intersection of the two valleys of lowest ascent at ($\sigma_{\mathrm{C}} = 2.06$ Å, $\sigma_{\mathrm{A}} = 3.94$ Å). This point constitutes a good compromise between the two optimization objectives. To test the reliability of the employed interpolation procedure, OPAS simulations (for the water activity curve) and standard MC simulations in the NpT ensemble (for the liquid solution densities) were carried out with the parameter

combination at that intersection point. The results are shown in Fig. 8.

[Figure 8 about here.]

The agreement between the interpolated values and the results of the performed simulations is excellent, proving that the interpolation predicts the model behavior with high accuracy for both objectives. Furthermore, the simulation results and the experimental reference data are in excellent agreement. Also the result for the salt activity coefficient is good. It is hence possible to find a parameter combination which performs well for solution densities as well as for activity data. There is good reason to expect that this can also be achieved for all other alkali halide salts in the concentration range studied here, at least if only models for the individual salts are needed. The idea can be extended for the improvement of the entire ion model set. However, the optimization task then becomes more complex due to the interconnections between the results of different salts containing the same ions. Furthermore, only a subset of the complete parameter space is studied here (ϵ was not varied) and it might be advantageous to use additional training data, such as structural or transport properties. We leave all this to future work.

The results of this feasibility study can also be interpreted by means of the Pareto set. The Pareto set contains all optimal solutions (here: optimal models) for which a gain in one of the objective functions cannot be attained without a loss in at least one of the other objective functions. Pareto optimal solutions are therefore best compromises. None of the solutions is to be preferred *a priori*. For a more comprehensive discussion of multicriteria optimization of molecular models, the reader is referred to refs.[41–43] The Pareto set of the present optimization task was obtained by eliminating the dominated models from the set of all sampled grid points. It is shown in Fig. 9, right panel.

[Figure 9 about here.]

As the present optimization task has two objective functions, the Pareto set is a one-dimensional object, i.e. a line. The shape of the Pareto set shows that accuracy for the

slope of the density can be gained while losing only little in the accuracy of the water activity. The left panel of Fig. 9 shows the picture of the Pareto set in parameter space, i.e. the parameter combinations that yield Pareto optimal solutions. In the present study, the picture of the Pareto set in parameter space is equal to the union of the white curves in Fig. 7, restricted to the path between the two global minima for each individual objective function. Similar results were also found by Stöbener et al. in their systematic investigation of the LJ model fluid.[41] The resulting branched structure can be clearly seen in both panels of Fig. 9. The model at the intersection of both branches corresponds to the Pareto knee (cf. right panel), which is known to be a good overall compromise for many optimization problems in practice.[41–43] This model was investigated in Fig. 8, and it is obvious why it performed excellently for both objectives.

4 Conclusion

A computational study of activities in aqueous solutions of the alkali halide salts at low to intermediate concentrations was carried out. The ion model set of Reiser et al.[11] was used for that purpose. The recently developed OPAS method for the computation of solvent activities was successfully used and validated against other simulation techniques. All results for activities from the present work are predictions based on a very simple ion model set which only has 10 parameters and describes many other properties of aqueous alkali halide solutions well. The predictions for the activities are good in many cases for the salts containing bromide or iodide. Poor results are observed especially for salts containing fluoride. However, there is ample room for improvements by reparameterization. A multi-objective approach should be used for this.

A strategy for model reparametrization is explored, using the OPAS results of the current ion model set. As an example of that strategy, the model for KF was optimized with respect to the solution densities as well as the water activity curve. For both objectives,

good agreement could be achieved in the concentration range studied here. Optimizing one salt model is, however, a much simpler task than optimizing an entire ion model set. The approach presented here for KF will be extended to the entire family of ion models of Reiser et al. in future work.

Acknowledgments

The present work was conducted under the auspices of the Boltzmann-Zuse Society of Computational Molecular Engineering (BZS) and the simulations were carried out on the Regional University Computing Center Kaiserslautern (RHRK) under the grant TUKL-MSWS as well as the High Performance Computing Center Stuttgart (HLRS) under the grant MMHBF. The authors would like to thank Steffen Reiser for fruitful discussions.

A Simulation Details

All simulations of this study were carried out with an extended version of the molecular simulation program $ms2$.[37] In $ms2$, thermophysical properties can be determined for rigid molecular models using Monte Carlo (MC) or molecular dynamics (MD) simulation techniques. For all simulations, the LJ interaction partners are determined for every time step and MC loop, respectively. Interaction energies between molecules and/or ions are determined explicitly for distances smaller than the cut-off radius r_{cut}. The thermostat incorporated in $ms2$ is velocity scaling. The pressure is kept constant using Andersen's barostat in MD, and random volume changes evaluated according to Metropolis acceptance criterion in MC, respectively. The simulation uncertainties are estimated with the block average method by Flyvbjerg and Petersen,[38] with a block length of 1,000 MD steps.

The total number of particles was 4000 throughout. In all MD simulations, Newton's equations of motion were solved with a gear predictor-corrector scheme of fifth order and a time step of $\Delta t = 1.2$ fs. The long-range interactions were considered by Ewald summation.[44]

The real space cut-off was equal to the LJ cut-off distance of 15 Å.

The OPAS simulations[31] were conducted as follows: At first, simulations in a modified isothermal-isobaric (NpT) ensemble were carried out. A physically reasonable configuration was obtained after equilibrating for 2,000,000 time steps, followed by a production run of 5,000,000 time steps. The resulting box volume V was then used for a run in the canonical (NVT) ensemble, in which equilibration and production took 3,000,000 and 10,000,000 time steps, respectively.

MC simulations in the isothermal-isobaric ensemble at a constant pressure of 1 bar were carried out to compute the density of aqueous KF solutions, using a total of $N = 1000$ particles. A physically reasonable configuration was obtained after 5,000 equilibration loops in the NVT ensemble, followed by 80,000 relaxation loops in the NpT ensemble. Thermodynamic averages were obtained by sampling 512,000 loops. Each loop consisted of $N_{\mathrm{NDF}}/3$ steps, where N_{NDF} indicates the total number of mechanical degrees of freedom of the system.

Funding Statement

The authors gratefully acknowledge financial support within the Reinhart Koselleck Program of the German Research Foundation (DFG).

Supporting Information

Supporting Information available: The results of OPAS simulations presented in Figs. 1 to 5 are tabulated in the Supporting Information.

References

(1) Hamer, W. J.; Wu, Y.-C. Osmotic Coefficients and Mean Activity Coefficients of Uni-univalent Electrolytes in Water at 25 °C. *J. Phys. Chem. Ref. Data* **1972**, *1*, 1047–1100.

(2) Nezbeda, I.; Moucka, F.; Smith, W. R. Recent Progress in Molecular Simulation of Aqueous Electrolytes: Force Fields, Chemical Potentials and Solubility. *Mol. Phys.* **2016**, *114*, 1665–1690.

(3) Joung, I. S.; Cheatham, T. E., III Determination of Alkali and Halide Monovalent Ion Parameters for Use in Explicitly Solvated Biomolecular Simulations. *J. Phys. Chem. B* **2008**, *112*, 9020–9041.

(4) Horinek, D.; Mamatkulov, S. I.; Netz, R. R. Rational Design of Ion Force Fields Based on Thermodynamic Solvation Properties. *J. Chem. Phys.* **2009**, *130*, 124507.

(5) Reif, M. M.; Huenenberger, P. H. Computation of Methodology-independent Single-ion Solvation Properties from Molecular Simulations. IV. Optimized Lennard-Jones Interaction Parameter Sets for the Alkali and Halide Ions in Water. *J. Chem. Phys.* **2011**, *134*, 144104.

(6) Gee, M. B.; Cox, N. R.; Jiao, Y.; Bentenitis, N.; Weerasinghe, S.; Smith, P. E. A Kirkwood-Buff Derived Force Field for Aqueous Alkali Halides. *J. Chem. Theory Comput.* **2011**, *7*, 1369–1380.

(7) Fyta, M.; Kalcher, I.; Dzubiella, J.; Vrbka, L.; Netz, R. R. Ionic Force Field Optimization Based on Single-ion and Ion-pair Solvation Properties. *J. Chem. Phys.* **2010**, *132*, 024911.

(8) Fyta, M.; Netz, R. R. Ionic Force Field Optimization Based on Single-ion and Ion-pair Solvation Properties: Going Beyond Standard Mixing Rules. *J. Chem. Phys.* **2012**, *136*, 124103.

(9) Fyta, M. Structural and Technical Details of the Kirkwood-Buff Integrals from the Optimization of Ionic Force Fields: Focus on Fluorides. *Eur. Phys. J. E* **2012**, *35*, 21.

(10) Deublein, S.; Vrabec, J.; Hasse, H. A Set of Molecular Models for Alkali and Halide Ions in Aqueous Solution. *J. Chem. Phys.* **2012**, *136*, 084501.

(11) Reiser, S.; Deublein, S.; Vrabec, J.; Hasse, H. Molecular Dispersion Energy Parameters for Alkali and Halide Ions in Aqueous Solution. *J. Chem. Phys.* **2014**, *140*, 044504.

(12) Luo, Y.; Roux, B. Simulation of Osmotic Pressure in Concentrated Aqueous Salt Solutions. *J. Phys. Chem. Lett.* **2010**, *1*, 183–189.

(13) Luo, Y.; Jiang, W.; Yu, H.; MacKerell, A. D., Jr.; Roux, B. Simulation Study of Ion Pairing in Concentrated Aqueous Salt Solutions with a Polarizable Force Field. *Faraday Discuss.* **2013**, *160*, 135–149.

(14) Saxena, A.; Garcia, A. E. Multisite Ion Model in Concentrated Solutions of Divalent Cations (MgCl2 and CaCl2): Osmotic Pressure Calculations. *J. Phys. Chem. B* **2015**, *119*, 219–227.

(15) Sanz, E.; Vega, C. Solubility of KF and NaCl in Water by Molecular Simulation. *J. Chem. Phys.* **2007**, *126*, 014507.

(16) Aragones, J. L.; Sanz, E.; Vega, C. Solubility of NaCl in Water by Molecular Simulation Revisited. *J. Chem. Phys.* **2012**, *136*, 244508.

(17) Joung, I. S.; Cheatham, T. E., III Molecular Dynamics Simulations of the Dynamic and Energetic Properties of Alkali and Halide Ions Using Water-Model-Specific Ion Parameters. *J. Phys. Chem. B* **2009**, *113*, 13279–13290.

(18) Paluch, A. S.; Jayaraman, S.; Shah, J. K.; Maginn, E. J. A Method for Computing the Solubility Limit of Solids: Application to Sodium Chloride in Water and Alcohols. *J. Chem. Phys.* **2012**, *137*, 039901.

(19) Moucka, F.; Nezbeda, I.; Smith, W. R. Molecular Force Fields for Aqueous Electrolytes:

SPC/E-compatible Charged LJ Sphere Models and Their Limitations. *J. Chem. Phys.* **2013**, *138*, 154102.

(20) Moucka, F.; Nezbeda, I.; Smith, W. R. Molecular Simulation of Aqueous Electrolytes: Water Chemical Potential Results and Gibbs-Duhem Equation Consistency Tests. *J. Chem. Phys.* **2013**, *139*, 124505.

(21) Moucka, F.; Nezbeda, I.; Smith, W. R. Molecular Force Field Development for Aqueous Electrolytes: 1. Incorporating Appropriate Experimental Data and the Inadequacy of Simple Electrolyte Force Fields Based on Lennard-Jones and Point Charge Interactions with Lorentz-Berthelot Rules. *J. Chem. Theory Comput.* **2013**, *9*, 5076–5085.

(22) Moucka, F.; Nezbeda, I.; Smith, W. R. Chemical Potentials, Activity Coefficients, and Solubility in Aqueous NaCl Solutions: Prediction by Polarizable Force Fields. *J. Chem. Theory Comput.* **2015**, *11*, 1756–1764.

(23) Mester, Z.; Panagiotopoulos, A. Z. Mean Ionic Activity Coefficients in Aqueous NaCl Solutions from Molecular Dynamics Simulations. *J. Chem. Phys.* **2015**, *142*, 044507.

(24) Orozco, G. A.; Moultos, O. A.; Jiang, H.; Economou, I. G.; Panagiotopoulos, A. Z. Molecular Simulation of Thermodynamic and Transport Properties for the H2O+NaCl System. *J. Chem. Phys.* **2014**, *141*, 234507.

(25) Jiang, H.; Mester, Z.; Moultos, O. A.; Economou, I. G.; Panagiotopoulos, A. Z. Thermodynamic and Transport Properties of H2O + NaCl from Polarizable Force Fields. *J. Chem. Theory Comput.* **2015**, *11*, 3802–3810.

(26) Benavides, A. L.; Aragones, J. L.; Vega, C. Consensus on the Solubility of NaCl in Water from Computer Simulations Using the Chemical Potential Route. *J. Chem. Phys.* **2016**, *144*, 124504.

(27) Mester, Z.; Panagiotopoulos, A. Z. Temperature-dependent Solubilities and Mean Ionic Activity Coefficients of Alkali Halides in Water from Molecular Dynamics Simulations. *J. Chem. Phys.* **2015**, *143*, 044505.

(28) Berendsen, H.; Grigera, J.; Straatsma, T. The Missing Term in Effective Pair Potentials. *J. Phys. Chem.* **1987**, *91*, 6269–6271.

(29) Reiser, S.; Horsch, M.; Hasse, H. Density of Methanolic Alkali Halide Salt Solutions by Experiment and Molecular Simulation. *J. Chem. Eng. Data* **2015**, *60*, 1614–1628.

(30) Reiser, S.; Horsch, M.; Hasse, H. Density of Ethanolic Alkali Halide Salt Solutions by Experiment and Molecular Simulation. *Fluid Phase Equilib.* **2016**, *408*, 141–150.

(31) Kohns, M.; Reiser, S.; Horsch, M.; Hasse, H. Solvent Activity in Electrolyte Solutions from Molecular Simulation of the Osmotic Pressure. *J. Chem. Phys.* **2016**, *144*, 084112.

(32) Lorentz, H. A. Ueber die Anwendung des Satzes vom Virial in der kinetischen Theorie der Gase. *Ann. Phys.* **1881**, *248*, 127–136.

(33) Berthelot, D. Sur le Melange des Gaz. *Comptes Rendus de l'Academie des Sciences Paris* **1898**, *126*, 1703–1706, 1857–1858.

(34) Murad, S.; Powles, J. A Computer-simulation of the Classic Experiment on Osmosis and Osmotic Pressure. *J. Chem. Phys.* **1993**, *99*, 7271–7272.

(35) Guevara-Carrion, G.; Vrabec, J.; Hasse, H. Prediction of Self-diffusion Coefficient and Shear Viscosity of Water and Its Binary Mixtures With Methanol and Ethanol by Molecular Simulation. *J. Chem. Phys.* **2011**, *134*, 074508.

(36) Smith, W. R.; Moucka, F.; Nezbeda, I. Osmotic Pressure of Aqueous Electrolyte Solutions via Molecular Simulations of Chemical Potentials: Application to NaCl. *Fluid Phase Equilib.* **2016**, *407*, 76–83.

(37) Glass, C. W.; Reiser, S.; Rutkai, G.; Deublein, S.; Koester, A.; Guevara-Carrion, G.; Wafai, A.; Horsch, M.; Bernreuther, M.; Windmann, T.; Hasse, H.; Vrabec, J. ms2: A Molecular Simulation Tool for Thermodynamic Properties, New Version Release. *Comput. Phys. Commun.* **2014**, *185*, 3302–3306.

(38) Flyvbjerg, H.; Petersen, H. Error-estimates on Averages of Correlated Data. *J. Chem. Phys.* **1989**, *91*, 461–466.

(39) Pitzer, K.; Peiper, J.; Busey, R. Thermodynamic Properties of Aqueous Sodium-Chloride Solutions. *J. Phys. Chem. Ref. Data* **1984**, *13*, 1–102.

(40) Reiser, S.; Horsch, M.; Hasse, H. Temperature Dependence of the Density of Aqueous Alkali Halide Salt Solutions by Experiment and Molecular Simulation. *J. Chem. Eng. Data* **2014**, *59*, 3434–3448.

(41) Stoebener, K.; Klein, P.; Reiser, S.; Horsch, M.; Kuefer, K. H.; Hasse, H. Multicriteria Optimization of Molecular Force Fields by Pareto Approach. *Fluid Phase Equilib.* **2014**, *373*, 100–108.

(42) Werth, S.; Stoebener, K.; Klein, P.; Kuefer, K.-H.; Horsch, M.; Hasse, H. Molecular Modelling and Simulation of the Surface Tension of Real Quadrupolar Fluids. *Chem. Eng. Sci.* **2015**, *121*, 110–117.

(43) Stoebener, K.; Klein, P.; Horsch, M.; Kuefer, K.; Hasse, H. Parametrization of Two-center Lennard-Jones plus Point-quadrupole Force Field Models by Multicriteria Optimization. *Fluid Phase Equilib.* **2016**, *411*, 33–42.

(44) Ewald, P. The Calculation of Optical and Electrostatic Grid Potential. *Ann. Phys.* **1921**, *64*, 253–287.

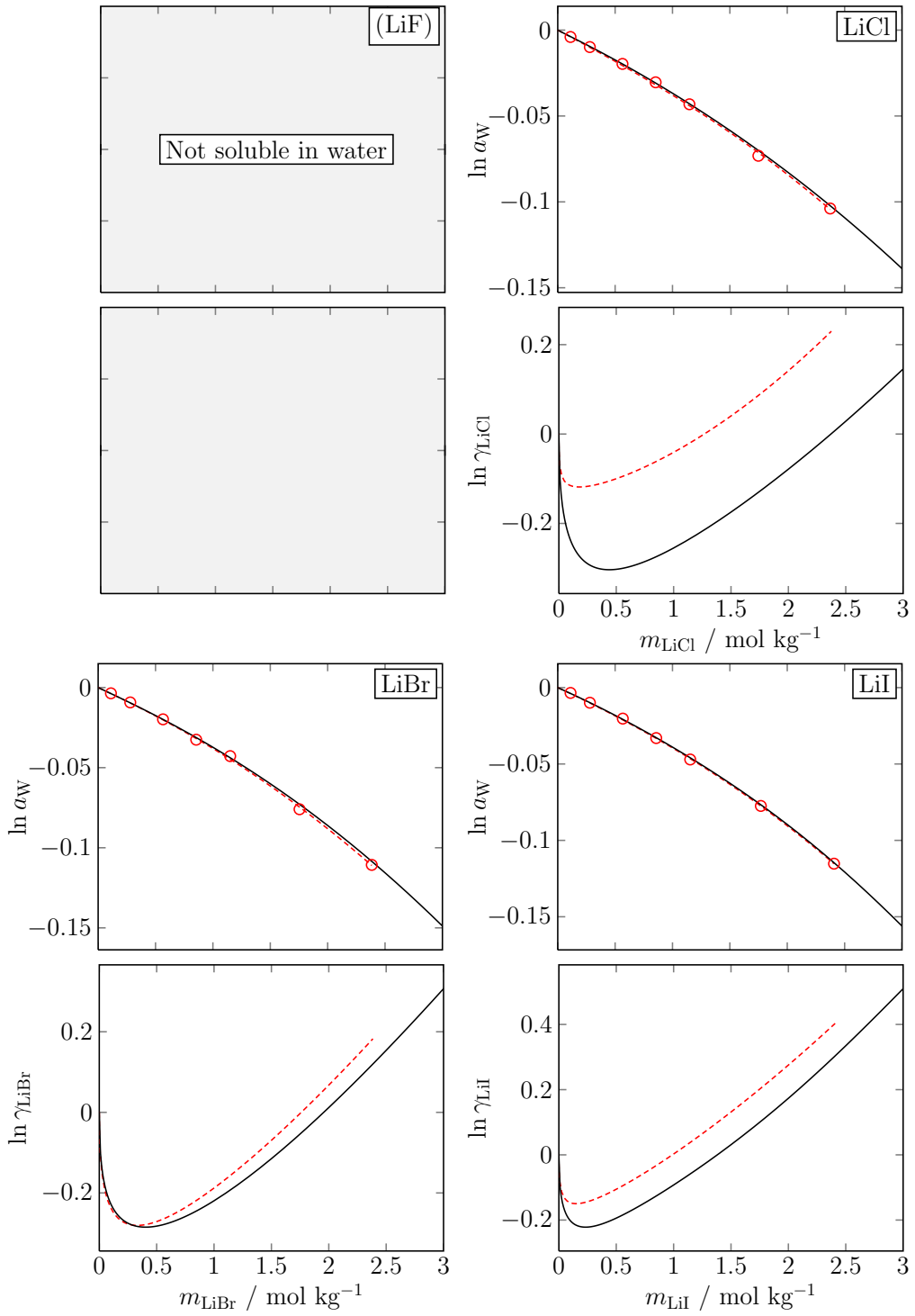

Figure 1: Water activities and salt activity coefficients over the salt molality for aqueous lithium halide solutions at $T = 298.15$ K. Present simulation results for the water activities are shown as red open circles, the statistical uncertainties are within symbol size, and the correlation to these results is shown as the red dashed line. The black line represents the correlation to experimental data by Hamer and Wu.[1] LiF is only soluble in traces and hence was not considered here.

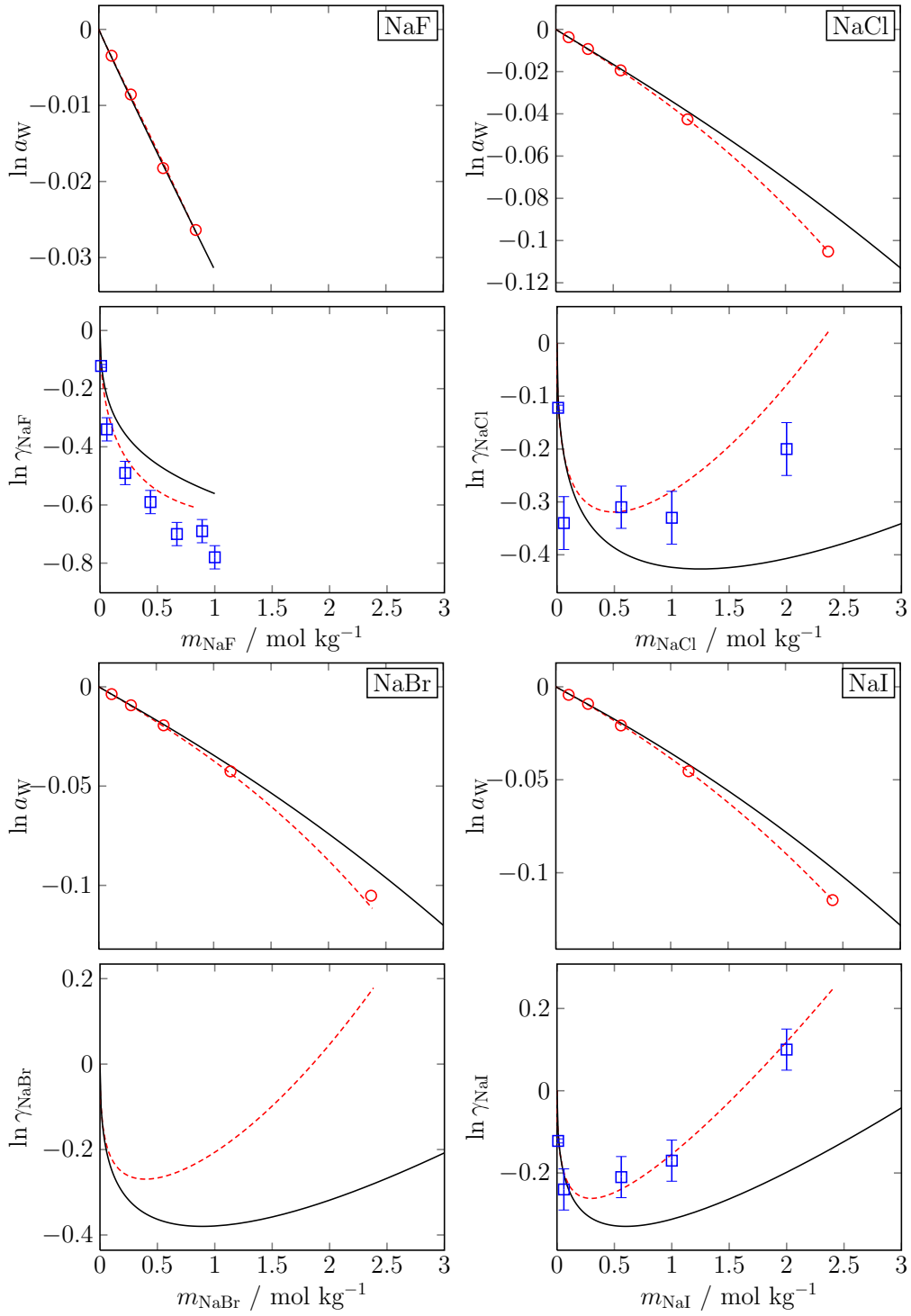

Figure 2: Water activities and salt activity coefficients over the salt molality for aqueous sodium halide solutions at $T = 298.15$ K. Present simulation results for the water activities are shown as red open circles, the statistical uncertainties are within symbol size, and the correlation to these results is shown as the red dashed line. The black line represents the correlation to experimental data by Hamer and Wu.[1] The blue squares show simulation results obtained by Mester and Panagiotopoulos[27] using the same molecular models.

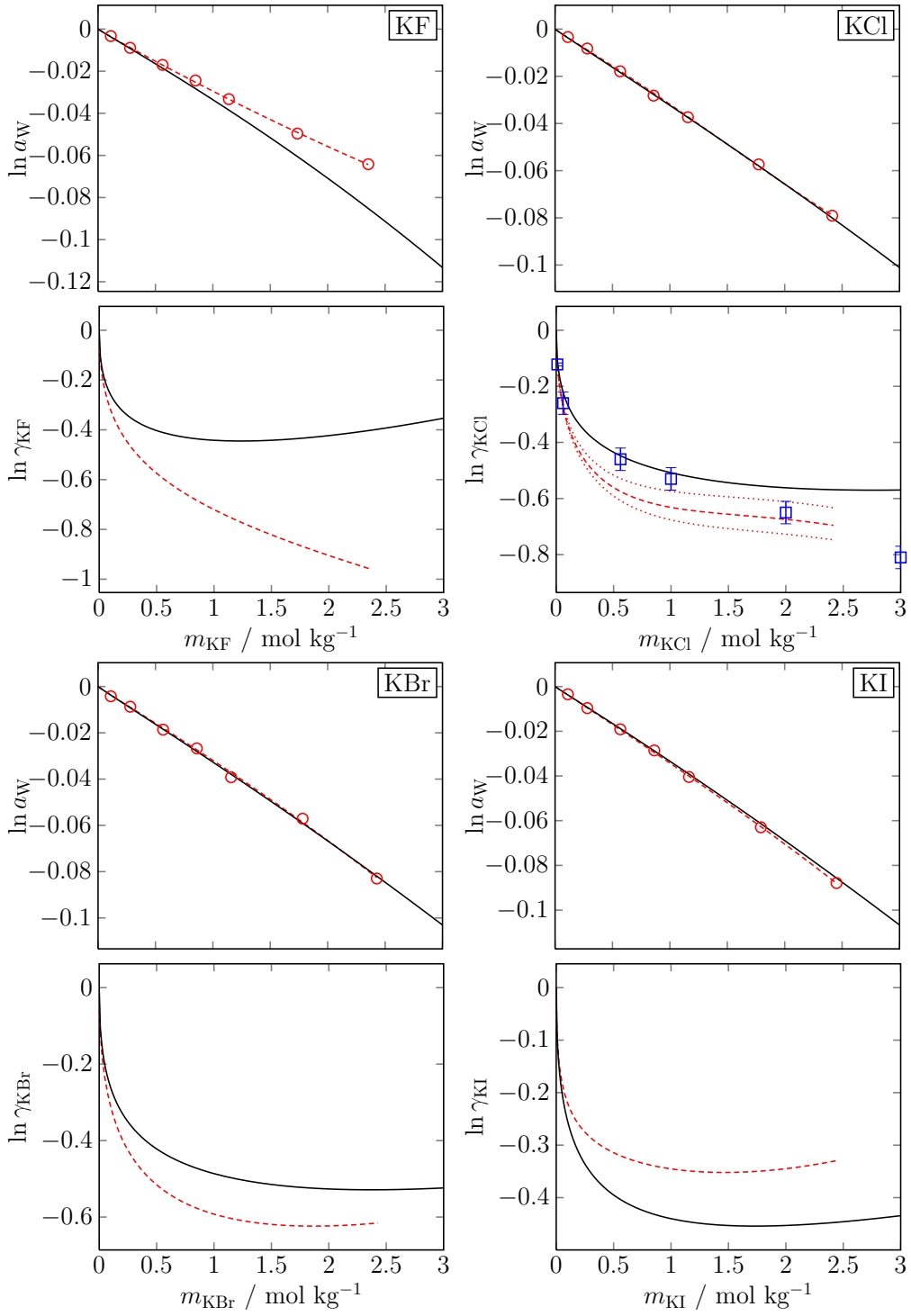

Figure 3: Water activities and salt activity coefficients over the salt molality for aqueous potassium halide solutions at $T = 298.15$ K. Present simulation results for the water activities are shown as red open circles, the statistical uncertainties are within symbol size, and the correlation to these results is shown as the red dashed line. The black line represents the correlation to experimental data by Hamer and Wu.[1] The blue squares show simulation results obtained by Mester and Panagiotopoulos[27] using the same molecular models. For KCl, the uncertainty in the correlation for $\ln \gamma_{KCl}$ is visualized by the red dotted lines.

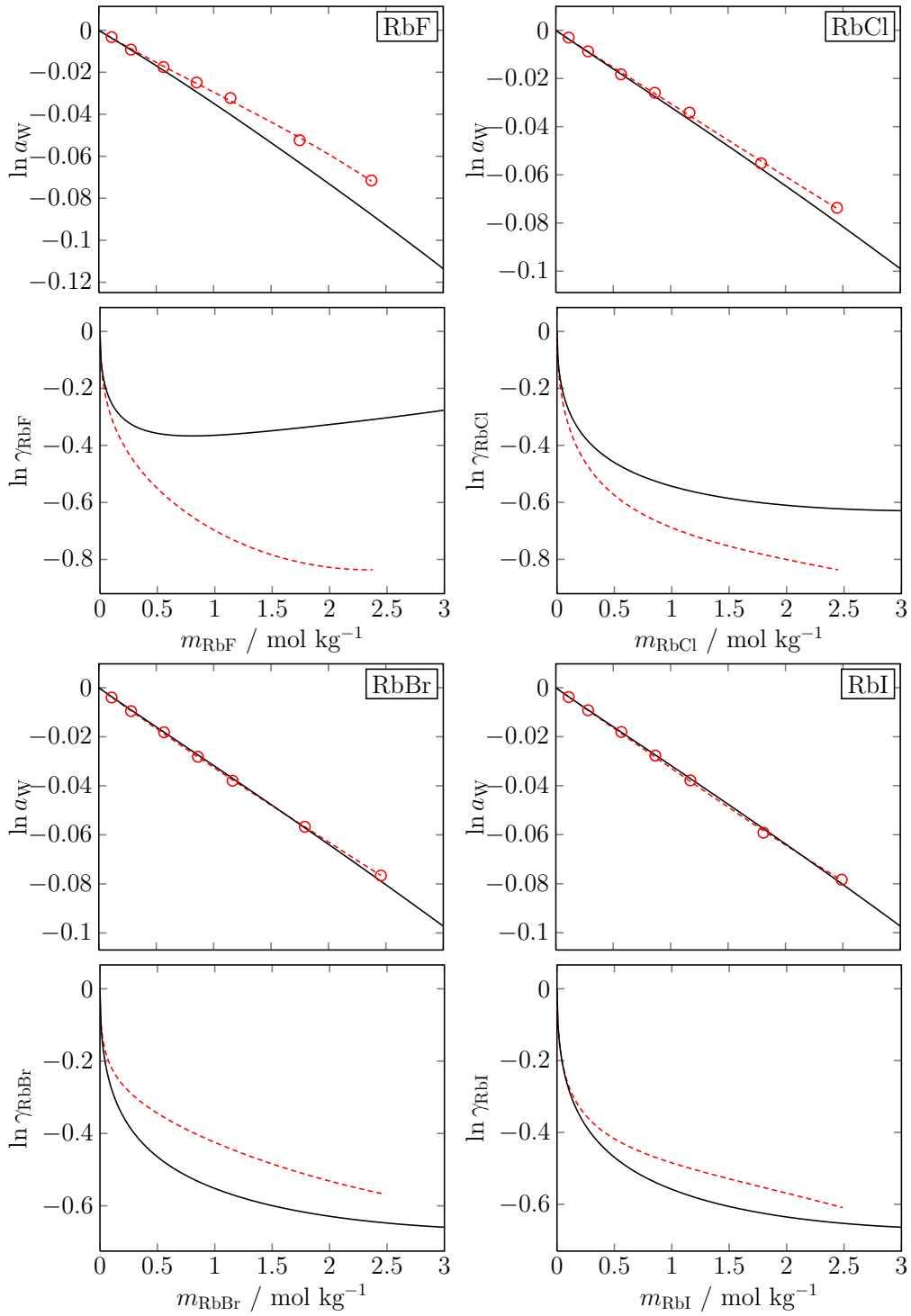

Figure 4: Water activities and salt activity coefficients over the salt molality for aqueous rubidium halide solutions at $T = 298.15$ K. Present simulation results for the water activities are shown as red open circles, the statistical uncertainties are within symbol size, and the correlation to these results is shown as the red dashed line. The black line represents the correlation to experimental data by Hamer and Wu.[1]

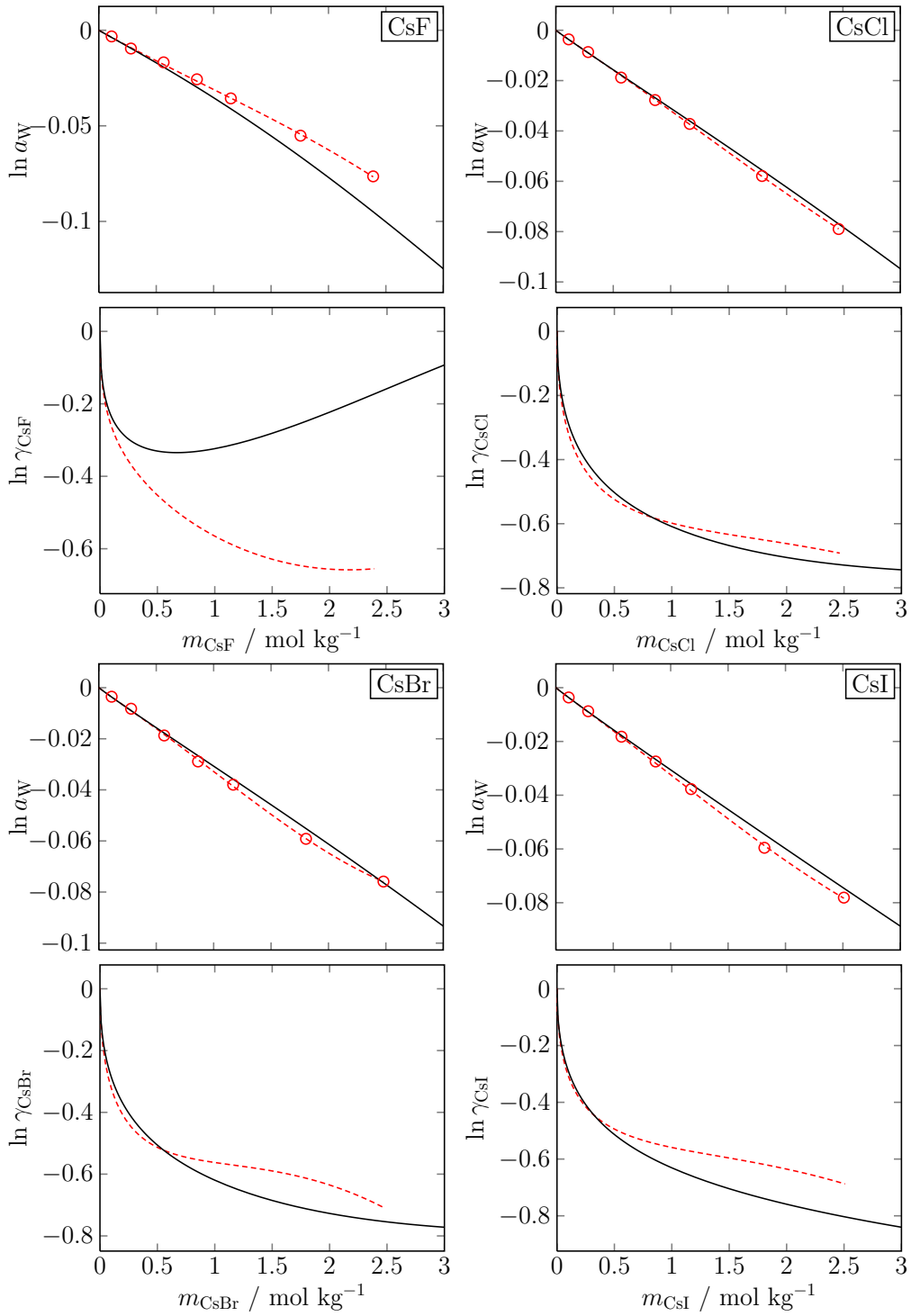

Figure 5: Water activities and salt activity coefficients over the salt molality for aqueous cesium halide solutions at $T = 298.15$ K. Present simulation results for the water activities are shown as red open circles, the statistical uncertainties are within symbol size, and the correlation to these results is shown as the red dashed line. The black line represents the correlation to experimental data by Hamer and Wu.[1]

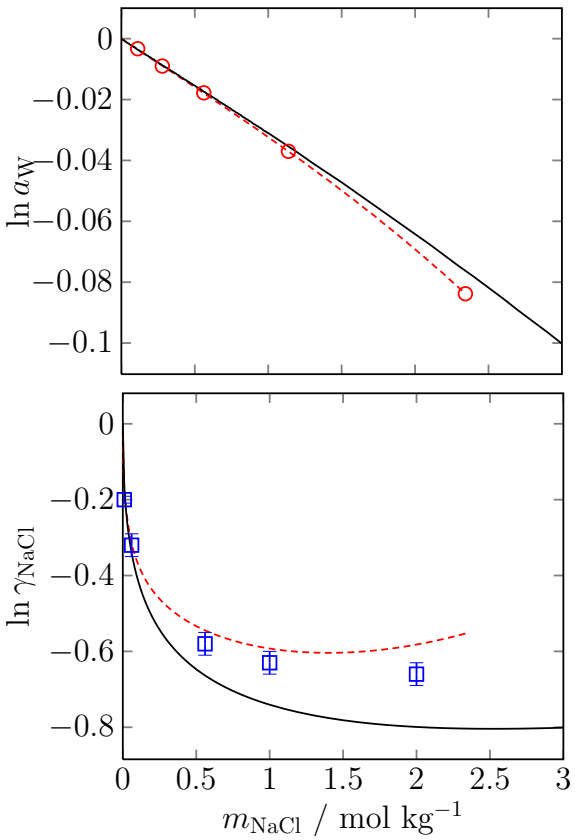

Figure 6: Water activities and salt activity coefficients over the salt molality for aqueous NaCl solutions at $T = 473.15$ K and $p' = 15.5$ bar (in the pure solvent phase). Present simulation results for the water activities are shown as red open circles, the statistical uncertainties are within symbol size, and the correlation to these results is shown as the red dashed line. The blue squares show simulation results obtained by Mester and Panagiotopoulos[27] using the same molecular models. The black line represents the correlation to experimental data by Pitzer et al.[39]

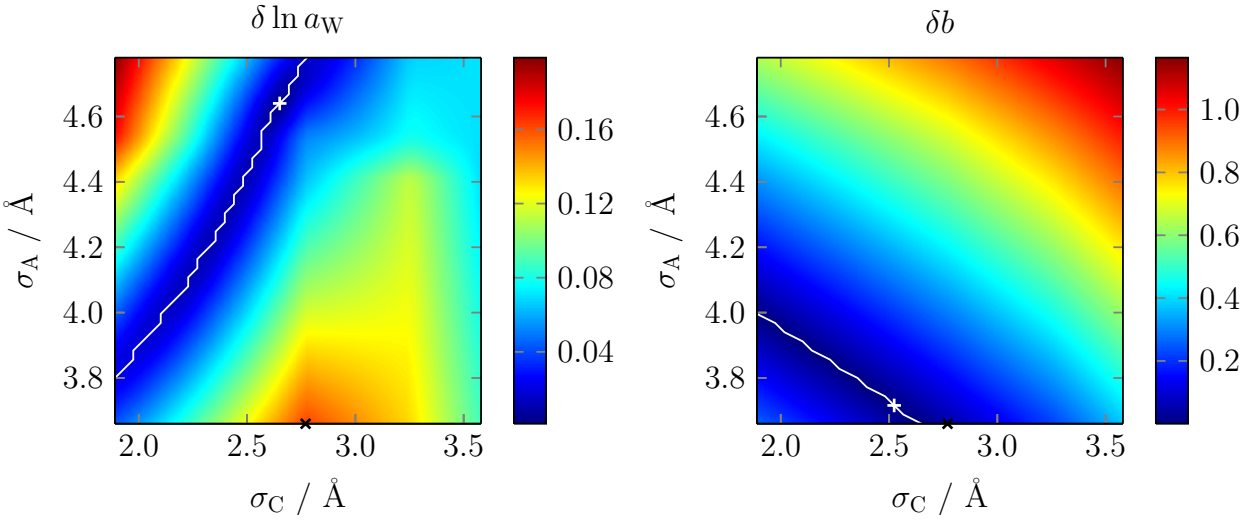

Figure 7: Deviation of the water activity curve, $\delta \ln a_W$ (left, at $T = 298.15$ K) and deviation of the slope of the density, δb (right, at $T = 293.15$ K) in the (σ_C, σ_A) parameter space for the design of a new KF model. The contours are estimated by linear interpolation of the correlated OPAS results and the density simulations of Reiser et al.,[40] respectively. The white lines indicate the valleys of lowest ascent/descent and hence represent the parameter combinations that are expected to perform well for the respective objective function. The white crosses along these lines show the location of the best possible model, i.e. the global minimum, for the respective property. The black cross shows the location of the KF model by Reiser et al.[11]

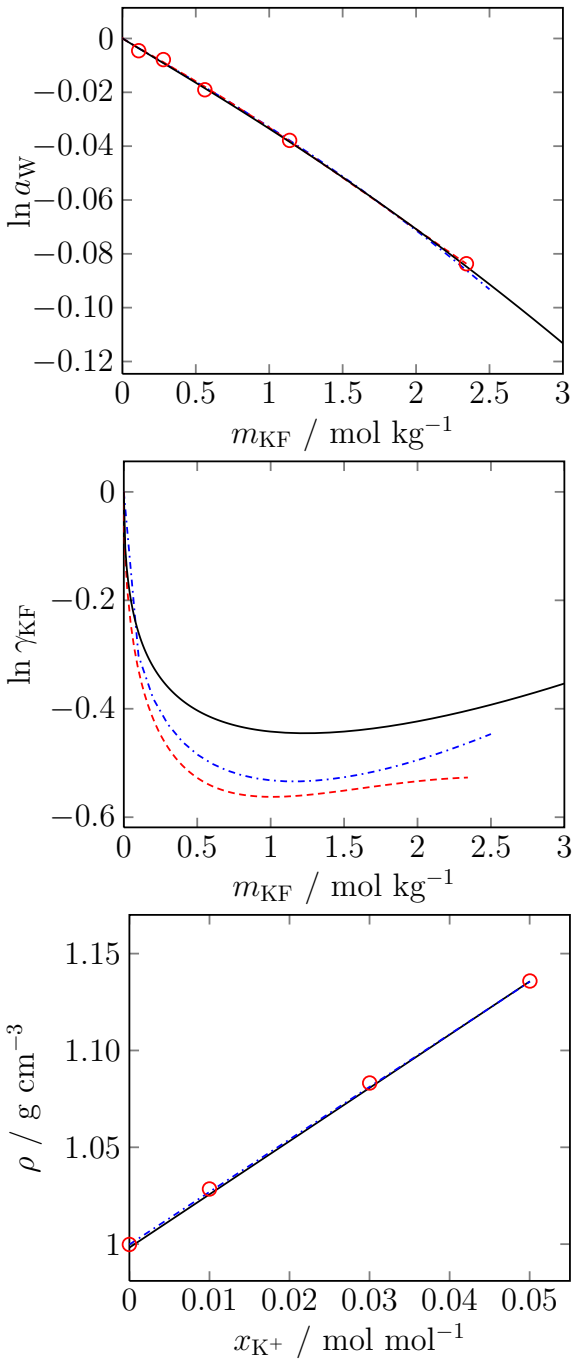

Figure 8: Water activity curve (top, at $T = 298.15$ K), activity coefficient of the salt (middle, at $T = 298.15$ K), and solution density (bottom, at $T = 293.15$ K) of aqueous solutions of KF. The black solid lines show the correlations to experimental data by Hamer and Wu[1] and by Reiser et al.,[40] respectively. The blue dash-dotted curves are obtained by the interpolation of OPAS results and the density simulations of Reiser et al.,[40] respectively. The red open circles show the actual simulation results using the model parameters ($\sigma_C = 2.06$ Å, $\sigma_A = 3.94$ Å), which agree with the curves predicted by interpolation. For the activities, the red dashed curves are correlations to actual simulation results. Note that the lines are only discernable for the salt activity coefficient.

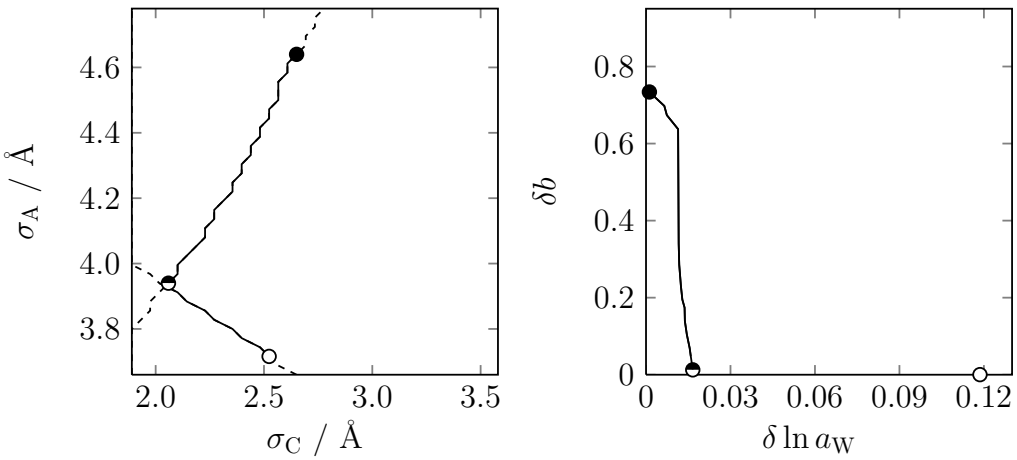

Figure 9: Set of Pareto optimal solutions for the design of a new KF model obtained by the interpolation of OPAS results as well as the density simulations of Reiser et al.[40] Left: Pareto set in parameter space. Right: Pareto set in objective function space. In the left panel, the dashed lines correspond to the valleys of lowest ascent/descent for an optimization task with a single objective function (cf. Fig. 7). The Pareto set shown as the solid lines is a subset of the union of these two valleys. The global minima for the two individual objectives are shown as the filled circle (water activity curve) and the open circle (slope of the density) and are equal to the white crosses in Fig. 7. The half-filled circle shows the model investigated in Fig. 8.

Table 1: Parameters of the ion model set by Reiser et al.[11] For all ions $\epsilon/k_{\mathrm{B}} = 200$ K.

Cation	σ/Å	Anion	σ/Å
Li^+	1.88	F^-	3.66
Na^+	1.89	Cl^-	4.41
K^+	2.77	Br^-	4.54
Rb^+	3.26	I^-	4.78
Cs^+	3.58		

Table 2: Fit parameters obtained by correlating the OPAS simulation results, $A = 0.5677$ throughout. The correlations are valid up to a molality of $m_{\mathrm{CA}} \approx 2.5$ mol kg^{-1} (except for NaF, for which the correlation is valid up to $m_{\mathrm{NaF}} \approx 1.0$ mol kg^{-1}). [a)] Not adjusted due to low solubility of NaF.

Salt	B	β	C
LiCl	7.4318	0.0335	0.0161
LiBr	1.7997	0.1145	0.0067
LiI	4.5988	0.0918	0.0108
NaF	0.6264	0.0783	0.0000 [a)]
NaCl	1.9013	0.0565	0.0176
NaBr	2.4399	0.0506	0.0248
NaI	1.9892	0.1146	0.0083
KF	0.9890	−0.0257	−0.0017
KCl	0.2732	0.2001	−0.0285
KBr	0.9387	0.0340	0.0016
KI	2.8092	−0.0076	0.0067
RbF	1.5008	−0.1015	0.0251
RbCl	0.6925	0.0434	−0.0072
RbBr	3.1791	−0.0547	0.0062
RbI	1.6667	0.0089	−0.0064
CsF	2.2560	−0.0955	0.0244
CsCl	0.6884	0.0931	−0.0167
CsBr	0.2888	0.2455	−0.0492
CsI	0.7946	0.0959	−0.0224

Graphic for Table of Contents use only

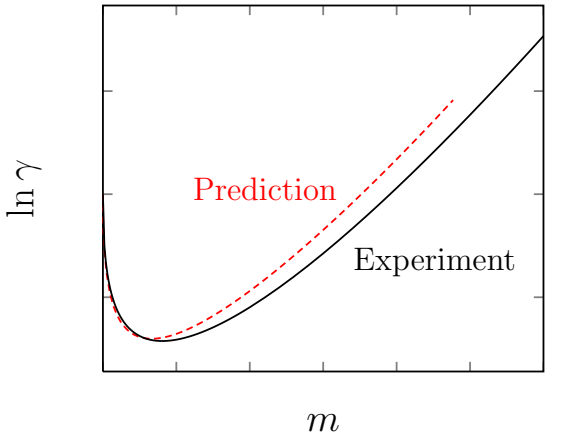

Supporting Information

Activities in Aqueous Solutions of the Alkali Halide Salts from Molecular Simulation

Maximilian Kohns, Michael Schappals, Martin Horsch,* and Hans Hasse

Laboratory of Engineering Thermodynamics, University of Kaiserslautern, Erwin-Schrödinger Str. 44, D-67663 Kaiserslautern, Germany

E-mail: martin.horsch@mv.uni-kl.de

The following tables contain the results of all OPAS simulations carried out in the present work. Uncertainties are given in parentheses, indicating one standard deviation of the mean.

*To whom correspondence should be addressed

Table S1: OPAS simulation results for lithium halides.

LiCl		
m / mol kg^{-1}	Π / MPa	$\ln a_{\mathrm{W}}$
0.1114(1)	0.55(3)	−0.0040(2)
0.2797(1)	1.35(5)	−0.0099(3)
0.5642(1)	0.70(7)	−0.0197(5)
0.8531(2)	4.16(8)	−0.0304(6)
1.1476(3)	5.9(1)	−0.0432(7)
1.7484(5)	10.0(1)	−0.073(1)
2.3744(7)	14.2(2)	−0.104(1)
LiBr		
m / mol kg^{-1}	Π / MPa	$\ln a_{\mathrm{W}}$
0.1113(1)	0.49(3)	−0.0036(2)
0.2800(1)	1.27(5)	−0.0093(4)
0.5653(2)	2.72(7)	−0.0198(5)
0.8545(3)	4.46(9)	−0.0326(7)
1.1505(5)	5.9(1)	−0.0428(9)
1.7548(8)	10.4(1)	−0.076(1)
2.384(1)	15.2(2)	−0.111(1)
LiI		
m / mol kg^{-1}	Π / MPa	$\ln a_{\mathrm{W}}$
0.1115(1)	0.48(3)	−0.0035(2)
0.2801(1)	1.36(5)	−0.0099(3)
0.5670(3)	2.78(7)	−0.0203(5)
0.8582(4)	4.52(9)	−0.0330(7)
1.1546(6)	6.4(1)	−0.0471(8)
1.770(1)	10.6(1)	−0.078(1)
2.407(1)	15.8(2)	−0.115(1)

Table S2: OPAS simulation results for sodium halides.

NaF		
m / mol kg^{-1}	Π / MPa	$\ln a_{\mathrm{W}}$
0.1112(1)	0.48(3)	−0.0035(2)
0.2786(1)	1.17(5)	−0.0086(4)
0.5598(1)	2.50(8)	−0.0182(6)
0.8440(3)	3.6(1)	−0.0264(8)
NaCl		
m / mol kg^{-1}	Π / MPa	$\ln a_{\mathrm{W}}$
0.1114(1)	0.51(3)	−0.0037(2)
0.2799(1)	1.27(4)	−0.0093(3)
0.5641(2)	2.66(7)	−0.0194(5)
1.1467(4)	5.8(1)	−0.0426(8)
2.371(1)	14.4(2)	−0.105(1)
NaBr		
m / mol kg^{-1}	Π / MPa	$\ln a_{\mathrm{W}}$
0.1113(1)	0.58(3)	−0.0042(2)
0.2798(1)	1.28(5)	−0.0093(3)
0.5647(2)	2.68(6)	−0.0196(4)
1.1496(4)	6.0(1)	−0.0440(7)
2.382(1)	15.3(2)	−0.112(1)
NaI		
m / mol kg^{-1}	Π / MPa	$\ln a_{\mathrm{W}}$
0.1114(1)	0.59(3)	−0.0043(3)
0.2804(1)	1.26(5)	−0.0092(3)
0.5666(2)	2.85(8)	−0.0208(6)
1.1557(6)	6.2(1)	−0.0454(8)
2.410(2)	15.7(2)	−0.115(1)

Table S3: OPAS simulation results for potassium halides.

KF		
m / mol kg^{-1}	Π / MPa	$\ln a_{\mathrm{W}}$
0.1113(1)	0.45(3)	−0.0033(2)
0.2793(1)	1.22(5)	−0.0089(3)
0.5620(1)	2.33(7)	−0.0170(5)
0.8488(2)	3.34(8)	−0.0244(6)
1.1395(3)	4.6(1)	−0.0333(7)
1.7360(7)	6.8(1)	−0.0496(9)
2.3536(9)	8.8(1)	−0.064(1)
KCl		
m / mol kg^{-1}	Π / MPa	$\ln a_{\mathrm{W}}$
0.1114(1)	0.46(3)	−0.0034(2)
0.2805(1)	1.13(4)	−0.0082(3)
0.5664(2)	2.45(7)	−0.0179(5)
0.8580(4)	3.86(8)	−0.0282(6)
1.1572(5)	5.1(1)	−0.0373(7)
1.773(1)	7.9(1)	−0.0574(9)
2.414(2)	10.8(1)	−0.079(1)
KBr		
m / mol kg^{-1}	Π / MPa	$\ln a_{\mathrm{W}}$
0.1114(1)	0.58(3)	−0.0042(2)
0.2806(1)	1.20(4)	−0.0087(3)
0.5670(2)	2.55(6)	−0.0186(4)
0.8602(4)	3.66(8)	−0.0267(6)
1.1590(5)	5.4(1)	−0.0392(7)
1.782(1)	7.8(1)	−0.0571(9)
2.428(2)	11.4(1)	−0.083(1)
KI		
m / mol kg^{-1}	Π / MPa	$\ln a_{\mathrm{W}}$
0.1115(1)	0.48(3)	−0.0035(2)
0.2808(1)	1.32(4)	−0.0097(3)
0.5681(2)	2.626)	−0.0191(4)
0.8643(5)	3.91(7)	−0.0286(5)
1.1665(7)	5.5(1)	−0.0404(7)
1.793(1)	8.6(1)	−0.0630(9)
2.452(2)	12.0(1)	−0.088(1)

Table S4: OPAS simulation results for rubidium halides.

RbF		
m / mol kg^{-1}	Π / MPa	$\ln a_{\mathrm{W}}$
0.1113(1)	0.45(3)	−0.0033(2)
0.2796(1)	1.27(4)	−0.0092(3)
0.5633(1)	2.40(7)	−0.0175(5)
0.8519(3)	3.40(8)	−0.0249(6)
1.1463(4)	4.4(1)	−0.0323(7)
1.7490(6)	7.2(1)	−0.0524(9)
2.375(1)	9.8(1)	−0.072(1)
RbCl		
m / mol kg^{-1}	Π / MPa	$\ln a_{\mathrm{W}}$
0.1115(1)	0.42(3)	−0.0031(2)
0.2806(1)	1.20(4)	−0.0088(3)
0.5675(2)	2.50(6)	−0.0183(5)
0.8619(4)	3.56(7)	−0.0260(5)
1.1639(6)	4.7(1)	−0.0342(6)
1.788(1)	7.6(1)	−0.0552(9)
2.448(2)	10.1(1)	−0.074(1)
RbBr		
m / mol kg^{-1}	Π / MPa	$\ln a_{\mathrm{W}}$
0.1115(1)	0.55(3)	−0.0040(2)
0.2805(1)	1.31(4)	−0.0096(3)
0.5684(2)	2.49(6)	−0.0182(4)
0.8629(4)	3.86(8)	−0.0282(6)
1.1649(7)	5.2(1)	−0.0379(7)
1.794(1)	7.7(1)	−0.0567(8)
2.457(3)	10.5(1)	−0.0766(9)
RbI		
m / mol kg^{-1}	Π / MPa	$\ln a_{\mathrm{W}}$
0.1116(1)	0.52(3)	−0.0038(2)
0.2810(1)	1.26(5)	−0.0092(4)
0.5703(3)	2.48(7)	−0.0181(5)
0.8671(5)	3.80(8)	−0.0277(6)
1.1714(8)	5.2(1)	−0.0378(6)
1.808(2)	8.1(1)	−0.0592(8)
2.490(2)	10.7(1)	−0.078(1)

Table S5: OPAS simulation results for cesium halides.

CsF		
m / mol kg^{-1}	Π / MPa	$\ln a_{\mathrm{W}}$
0.1114(1)	0.44(3)	−0.0032(2)
0.2797(1)	1.31(4)	−0.0095(3)
0.5643(2)	2.30(6)	−0.0168(4)
0.8543(3)	3.51(8)	−0.0257(6)
1.1495(4)	4.9(1)	−0.0356(7)
1.7567(8)	7.6(1)	−0.0551(8)
2.389(1)	10.5(1)	−0.076(1)
CsCl		
m / mol kg^{-1}	Π / MPa	$\ln a_{\mathrm{W}}$
0.1115(1)	0.50(3)	−0.0036(2)
0.2811(1)	1.19(4)	−0.0087(3)
0.5685(2)	2.58(6)	−0.0188(5)
0.8644(4)	3.80(8)	−0.0277(6)
1.1658(7)	5.1(1)	−0.0372(7)
1.796(1)	7.9(1)	−0.0579(8)
2.463(2)	10.8(1)	−0.079(1)
CsBr		
m / mol kg^{-1}	Π / MPa	$\ln a_{\mathrm{W}}$
0.1116(1)	0.48(3)	−0.0035(2)
0.2811(1)	1.13(4)	−0.0082(3)
0.5694(3)	2.56(6)	−0.0187(5)
0.8640(5)	3.96(8)	−0.0289(6)
1.1701(7)	5.20(1)	−0.0380(7)
1.804(2)	8.2(1)	−0.0592(9)
2.479(2)	10.4(1)	−0.076(1)
CsI		
m / mol kg^{-1}	Π / MPa	$\ln a_{\mathrm{W}}$
0.1116(1)	0.50(3)	−0.0036(2)
0.2816(1)	1.20(4)	−0.0088(3)
0.5716(3)	2.50(6)	−0.0182(4)
0.8691(6)	3.76(8)	−0.0275(6)
1.1777(9)	5.2(1)	−0.0377(6)
1.816(2)	8.2(1)	−0.0596(8)
2.508(3)	10.7(1)	−0.078(1)

Table S6: OPAS simulation results for the aqueous NaCl solution at $T = 473.15$ K and $p' = 15.5$ bar (in the pure solvent phase).

m / mol kg^{-1}	Π / MPa	$\ln a_{\mathrm{W}}$
0.1112(1)	0.63(2)	−0.0033(1)
0.2789(1)	1.68(4)	−0.0090(2)
0.5612(3)	3.33(5)	−0.0178(3)
1.1377(5)	6.92(8)	−0.0370(4)
2.343(2)	15.6(1)	−0.0838(7)